Kinetics of the Formation of the 1,3-Complex and on the Formation and Decomposition of the Intermediate Complex. Reaction of 2,4,6-Trinitroanisole with n-Butylamine in Dimethyl Sulphoxide

Yoshinori Hasegawa
College of General Education, Tohoku University, Kawauchi, Sendai 980, Japan

The reaction of 2,4,6-trinitroanisole with n-butylamine in dimethyl sulphoxide occurs in three stages, which are observed separately by stopped-flow spectrophotometry. Stages I and II are the formation of the kinetically controlled 1,3-complex and the thermodynamically stable intermediate complex, respectively. Stage III is the decomposition of the intermediate. The mechanism of the formation and decomposition of the intermediate is indicated to be rapid equilibrium deprotonation of the zwitterionic complex followed by rate-limiting, general acid-catalysed leaving-group departure. The product is finally in equilibrium with both its conjugate base and its 1,3-complex from attack of n-butylamine.

N.m.r. spectroscopy has revealed that the reaction of 2,4,6-trinitroanisole (TNA) with methoxide ion in methanolic dimethyl sulphoxide (DMSO) initially produces the kinetically controlled 1,3-complex (**2**) which is subsequently converted into the thermodynamically controlled 1,1-complex (**1**).[1-4] Fyfe *et al.* obtained flow n.m.r. spectra in the reaction of TNA with n-butylamine in methanolic DMSO.[5] They have confirmed that the intermediate 1,1-complex (**3**) is formed on the reaction pathway and suggested that the 1,3-complex (**4**) is produced at the initial stage.

Bunnett and his co-workers have observed the formation of an intermediate complex in the reaction of 1-ethoxy-2,4-dinitronaphthalene with primary and cyclic secondary amines in DMSO and presented the overall reaction mechanism.[6,7] The mechanism is shown to involve rapid equilibrium deprotonation of the zwitterionic complex followed by general acid-catalysed leaving-group departure. This is direct evidence for the specific base–general acid (SB–GA) mechanism[8,9] of the aromatic nucleophilic substitution (S_NAr) reaction.

Recently, we have studied the kinetics of the reaction of methyl 4-methoxy-3,5-dinitrobenzoate with piperidine and n-butylamine in DMSO.[10,11] As regards the reaction of methyl 4-methoxy-3,5-dinitrobenzoate with n-butylamine, proton transfer between the zwitterionic complex (**5**) and its conjugate base (**6**) is rapid and the decomposition of the intermediate is first order in general acid.

To understand not only anionic σ-complex chemistry but the mechanism of the S_NAr reaction, it is of interest to study the kinetics of the reaction of TNA and n-butylamine. In this paper, we report the kinetics of this reaction in DMSO. The overall reaction is shown in Scheme 1.

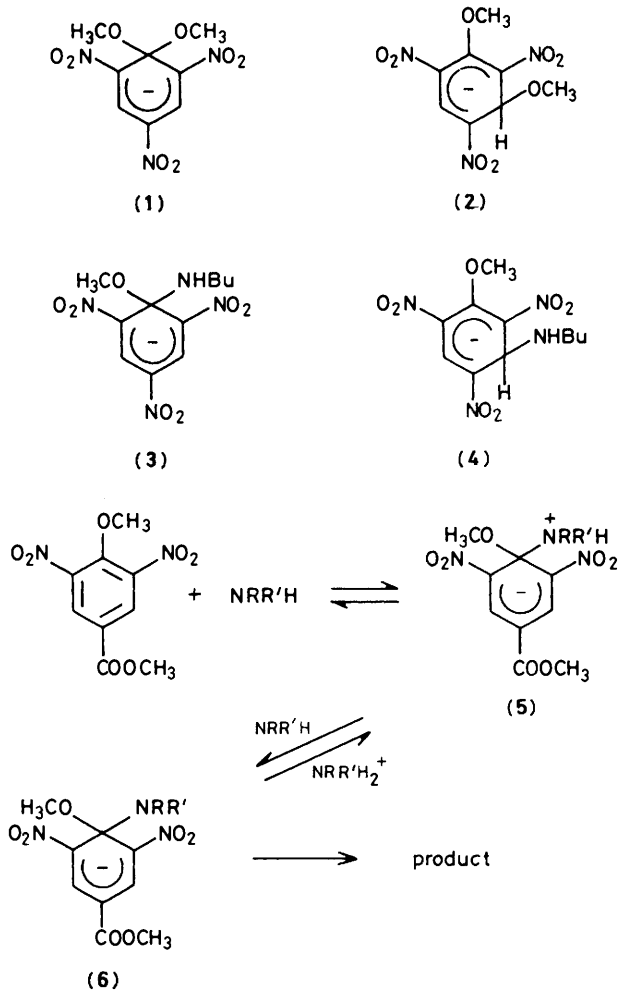

Results

General Features.—The reaction of TNA and n-butylamine in DMSO is rapid and somewhat complicated. However, it is revealed that the reaction occurs in three stages, which are observed separately by stopped-flow measurements. Representative stopped-flow traces are presented in Figure 1.

Trace 1a was observed in the presence of high concentration of n-butylamine and an adequate amount of n-butylamine hydrochloride. It is obvious that the initial (stage I) reaction is much faster than the following (stage II) reaction. Similar stopped-flow traces to 1a were obtained in the absence of n-butylamine hydrochloride. Stage II becomes predominant with a decrease of concentration of n-butylamine at a constant concentration of n-butylamine hydrochloride. When concentrations of n-butylamine are lower than 0.0040 at 0.0050M of n-butylamine hydrochloride, stage I is negligible and stopped-flow traces of stage II can be obtained alone; see trace 1d.

Fyfe *et al.* have observed the formation of the intermediate complex in methanolic DMSO by a flow n.m.r. technique and suggested that the 1,3-complex was formed at the initial stage.[5] Stages I and II are attributed to the formation of the 1,3-complex and intermediate complex, respectively.

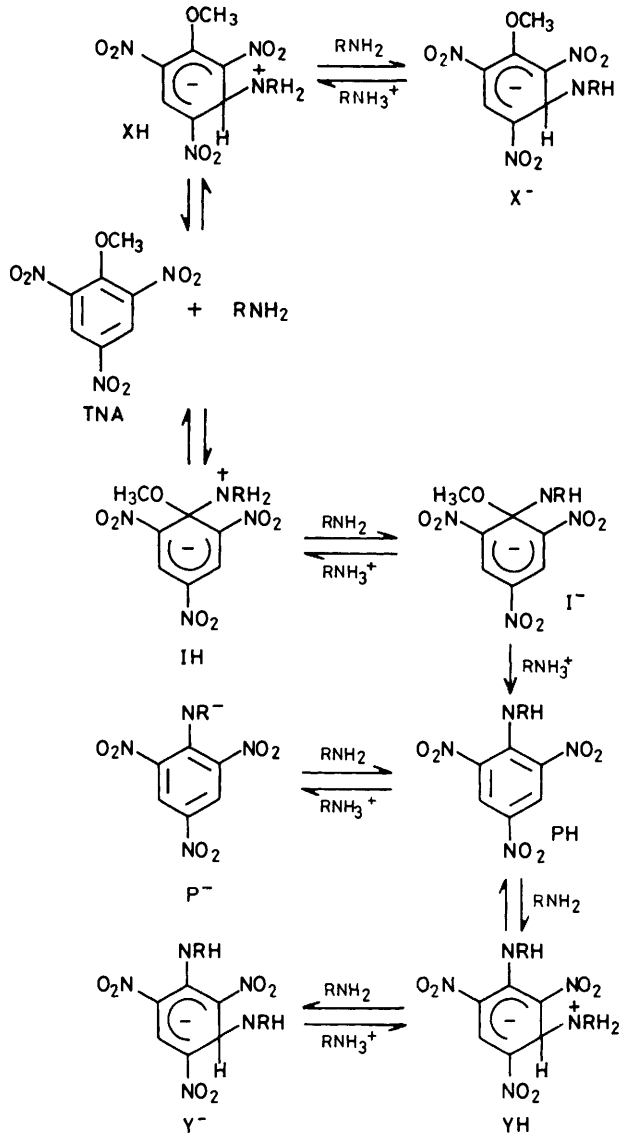

Scheme 1. RNH_2 = n-butylamine

Stage III is the decomposition of the intermediate complex; see trace 1c.

The final spectra of TNA in the presence of various concentrations of n-butylamine with constant concentration of n-butylamine hydrochloride are shown in Figure 2.

For comparison, we tried to observe the spectra of PH, a mixture of PH and n-butylamine in methanolic DMSO, and a mixture of PH and sodium hydroxide in aqueous DMSO (see spectra 2h—k). The absorption with $\lambda_{max.}$ 418 nm of spectrum 2i is assigned to the 1,3-complex Y^- formed from attack of n-butylamine by Fyfe *et al.*[5] The absorption at $\lambda_{max.}$ 442 and 500 nm of spectrum 2k is assignable to P^-.*

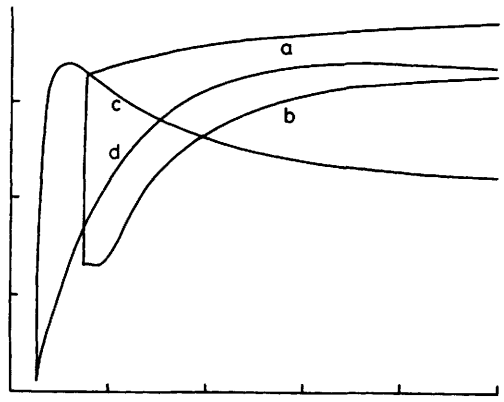

Figure 1. Representative stopped-flow traces of reaction of TNA (3.0×10^{-5}M) and n-butylamine (0.061M) with n-butylamine hydrochloride (0.0050M) in DMSO at 430 nm at 25 °C, a and b; stopped-flow traces of TNA (3.0×10^{-5}M) and n-butylamine (0.0040M) with n-butylamine hydrochloride (0.0050M), c and d. Vertical scale, ΔOD/div; a and b: 0.04 (cell length 2 mm), c and d: 0.2 (cell length 1 cm). Horizontal scale; a: 0.4 s/div, b: 4 ms/div, c: 10 s/div, d: 1 s/div

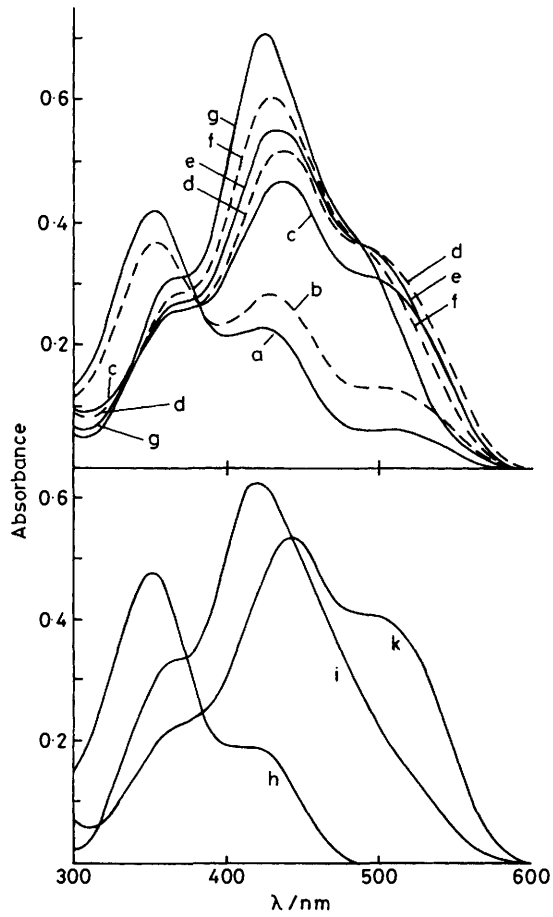

Figure 2. Spectra of TNA (3.0×10^{-5}M) with n-butylamine hydrochloride (0.0050M) in DMSO containing various concentrations of n-butylamine. [RNH_2]: a, 3.0×10^{-4}; b, 7.0×10^{-4}; c, 7.0×10^{-3}; d, 0.0101; e, 0.020; f, 0.041; g, 0.152M. Spectrum of PH (3.0×10^{-5}M) in DMSO: h; spectrum of PH (3.0×10^{-3}M) with n-butylamine (0.10M) in methanolic DMSO (50% methanol by volume): i; spectrum of PH (3.0×10^{-5}M) with sodium hydroxide (1.3×10^{-4}M) in aqueous DMSO (0.1% water by volume): k

* In the presence of low concentrations of sodium hydroxide, the spectrum of PH in DMSO containing a trace of water has an absorption at $\lambda_{max.}$ 442 and 500 nm. In the presence of high concentrations of sodium hydroxide, the spectrum of PH shows an absorption at $\lambda_{max.}$ 515 nm. This spectral behaviour is similar to that of *N*-methylpicramide with sodium methoxide in methanolic DMSO (5% methanol by volume) as reported in ref. 12. The absorption at $\lambda_{max.}$ 442 and 500 nm is assigned to P^- and that at $\lambda_{max.}$ 515 nm to the hydroxide adduct of P^-.

$$TNA + RNH_2 \underset{k_{-1}}{\overset{k_1}{\rightleftharpoons}} XH$$

$$XH + RNH_2 \underset{k_{-2}}{\overset{k_2}{\rightleftharpoons}} X^- + RNH_3^+$$

$$TNA + RNH_2 \underset{k_{-3}}{\overset{k_3}{\rightleftharpoons}} IH$$

$$IH + RNH_2 \underset{k_{-4}}{\overset{k_4}{\rightleftharpoons}} I^- + RNH_3^+$$

$$I^- + RNH_3^+ \xrightarrow{k_5} PH + RNH_2 + CH_3OH$$

$$PH + RNH_2 \overset{K_p}{\rightleftharpoons} P^- + RNH_3^+$$

$$PH + 2\,RNH_2 \overset{K_y}{\rightleftharpoons} Y^- + RNH_3^+$$

Scheme 2.

Spectra 2a—d were observed in the presence of low concentrations of n-butylamine at constant concentration of n-butylamine hydrochloride. From comparison with spectra 2h and k, the absorption at $\lambda_{max.}$ 350 nm is ascribed to the product PH and that with $\lambda_{max.}$ 435 and 500 nm to P^-. Assciated with conversion of PH into P^-, an isosbestic point appears at 382 nm.

When concentrations of n-butylamine are higher than 0.020M, a new species forms (see spectra 2e—g). By comparing spectra 2e—g with spectrum 2k of P^- and 2i of Y^-, it seems that spectra 2e—g are due to mixtures of P^- and Y^-. Thus, the new species is assignable to Y^-.

Procedure of Kinetic and Equilibrium Studies.—We rewrite Scheme 1 as 2. Kinetic and equilibrium studies of the stages I—III were made by a stopped-flow spectrophotometer. The product equilibrium was studied by spectrophotometric measurements.

Stage I. Equilibrium.—As shown in Figure 1a stage I is much faster than stage II. When stage I is taken into account, it can be treated as an independent equilibrium; see Figure 1b. An equilibrium constant for the overall conversion of TNA into X^- is defined by equation (1). It is known that an amine complex

$$K_x = \frac{[X^-][RNH_3^+]}{[TNA][RNH_2]^2} \quad (1)$$

exists predominantly as its conjugate base rather than as a zwitterionic complex[6,7,13] and therefore equation (1) can be rearranged to (2) where $[TNA]_0$, A, ε, and d are the

$$\frac{[TNA]_0}{A} = \frac{[RNH_3^+]}{K_x \varepsilon d[RNH_2]^2} + \frac{1}{\varepsilon d} \quad (2)$$

stoicheiometric TNA concentration, equilibrium absorbance, molar extinction coefficient, and path length of the cell used, respectively.

Measurements were made in the presence of both n-butylamine and n-butylamine hydrochloride in large excess of TNA. Stage 1 is very fast and proceeds to a non-negligible extent for the mixing time (1.5 ms). The equilibrium absorbance was obtained by extrapolating a kinetic trace against time back to zero time. Equilibrium data are displayed in Part A of Table 1. A plot of $[TNA]_0/A_{430}$ against $[RNH_2]^{-2}$ (Figure 3a) gives a straight line. ε_{430} and K_x are determined to be 19 500 l mol^{-1} cm^{-1} and 27 l mol^{-1}, respectively.

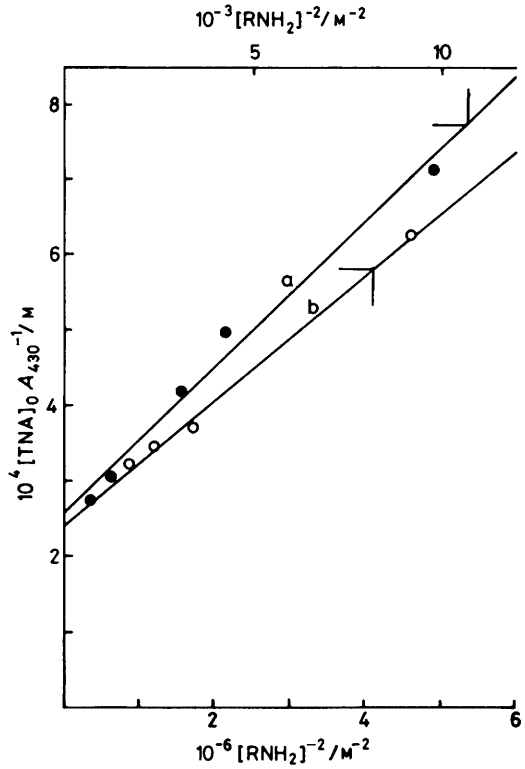

Figure 3. Plots of $[TNA]_0/A_{430}$ against $1/[RNH_2]^2$; a and b are from parts A and B of Table 1, respectively

Table 1. Reaction of TNA with n-butylamine. States I and II equilibria[a]

$[RNH_2]$/M	A_{430}[b]
Part A[c]	
0.0101	0.042
0.0152	0.060
0.0178	0.072
0.028	0.098
0.036	0.108
Part B[d]	
0.000 46	0.016
0.000 76	0.027
0.000 91	0.029
0.001 26	0.031

[a] Temperature: 25 °C; $[RNH_3Cl]$ 0.0050M. [b] Equilibrium absorbance at 430 nm; the path length of the cell used is 2 mm. [c] $[TNA]_0$ 3.0 × 10^{-5}M. [d] $[TNA]_0$ 1.0 × 10^{-5}M

Stage I. Kinetics.—The kinetics of stage I were carried out by two experiments. In the first experiment, concentrations of n-butylamine were varied in the absence of n-butylamine hydrochloride. In the second experiment, concentrations of n-butylamine were varied at constant concentration of n-butylamine hydrochloride.

In the first experiment, we may write equation (3) where AH^+ is the species formed from deprotonation of XH by n-butylamine and is equal in concentration to X^-. This represents a

$$TNA \underset{k_{r_2}}{\overset{k_{r_1}}{\rightleftharpoons}} X^- + AH^+ \quad (3)$$

mixed first-order (forward) and second-order (reverse) equilibrium process. The solution[14] for equation (3) is presented by (4), where $[X^-]$ and $[X^-]_e$ are concentrations of

$$\ln\left(\frac{[TNA]_0[X^-]_e + [X^-]([TNA]_0 - [X^-]_e)}{[TNA]_0([X^-]_e - [X^-])}\right) = \left(\frac{2[TNA]_0 - [X^-]_e}{[X^-]_e}\right)k_{f1}t \quad (4)$$

X^- during the reaction and at equilibrium respectively. When conversion of TNA into X^- is virtually complete, equation (4) simplifies to (5).

$$\ln\frac{[TNA]_0}{[TNA]_0 - [X^-]} = k_{f1}t \quad (5)$$

Using the steady-state approximation with respect to XH, k_{f1} is given by equation (6).

$$k_{f1} = \frac{k_1[RNH_2]k_2[RNH_2]}{k_{-1} + k_2[RNH_2]} \quad (6)$$

In Part A of Table 2, kinetic data are presented. Values of $k_{f1}/[RNH_2]$ are substantially constant and so proton transfer between XH and X^- is more rapid than the k_{-1} step. The value of k_1 ($= k_{f1}/[RNH_2]$) is 4 200 l mol^{-1} s^{-1}.

In the second experiment, both forward and reverse reactions are pseudo-first-order and so the observed rate constant, k_φ,* is the sum of the forward and reverse component. Again using the

$$TNA \underset{k_{r1}}{\overset{k_{f1}}{\rightleftharpoons}} X^- \quad (7)$$

$$k_\varphi = k_{f1} + k_{r1} \quad (8)$$

steady-state approximation, k_φ is given by equation (9). As proton transfer is rapid, k_φ is reduced to (10). Multiplying each side by $[RNH_2]$ gives (11). Rate data are presented in Part B of

$$k_\varphi = \frac{k_1[RNH_2]k_2[RNH_2] + k_{-1}k_{-2}[RNH_3^+]}{k_{-1} + k_2[RNH_2]} \quad (9)$$

$$k_\varphi = k_1[RNH_2] + \frac{k_{-1}k_{-2}[RNH_3^+]}{k_2[RNH_2]} \quad (10)$$

$$k_\varphi[RNH_2] = k_1[RNH_2]^2 + \frac{k_{-1}k_{-2}[RNH_3^+]}{k_2} \quad (11)$$

Table 2. A plot of $k_\varphi[RNH_2]$ against $[RNH_2]^2$ (Figure 4a) is linear. The slope, k_1, is 3 900 l mol^{-1} s^{-1}. As the intercept is 0.50 mol l^{-1} s^{-1}, $k_{-1}k_{-2}/k_2$ is 100 s^{-1}. From $K_x = k_1k_2/k_{-1}k_{-2}$, K_x is calculated to be 39 l mol^{-1}.

Stage II. Equilibrium and Kinetics.—Measurements were made under the conditions that concentrations of n-butylamine are lower than those of the previous case at constant concentration of n-butylamine hydrochloride.

Trace 1d of Figure 1 indicates that we can treat stage II as an independent equilibrium, neglecting state III. The equilibrium and kinetic treatment is the same as the previous case. The equilibrium constant, K_i, is defined by equation (12). Equilibrium and kinetic data are tabulated in Part B of Tables 1 and 3.

$$K_i = \frac{[I^-][RNH_3^+]}{[TNA][RNH_2]^2} \quad (12)$$

Table 2. Reaction of TNA with n-butylamine. Stage I kinetics[a]

$[RNH_2]$/M	k_{f1}/mol l^{-1}	$k_{f1}[RNH_2]^{-1}$/ l mol^{-1} s^{-1}	k_φ/s^{-1}
		Part A[b]	
0.0065	27	4 200	
0.0081	35	4 300	
0.0127[c]	50	3 900	
0.025	109	4 300	
0.051[c]	210	4 100	
0.065	280	4 300	
0.101	420	4 200	
		Part B[d]	
0.0101			94
0.0152			96
0.0178			99
0.028			119
0.030			129
0.036			157
0.046			189

[a] Temperature: 25 °C; measurements were made at 430 nm. [b] $[TNA]_0$ 3.0×10^{-5}M. [c] $[TNA]_0$ 1.0×10^{-5}M. [d] $[TNA]_0$ 3.0×10^{-5}M; $[RNH_3Cl]$ 0.0050M.

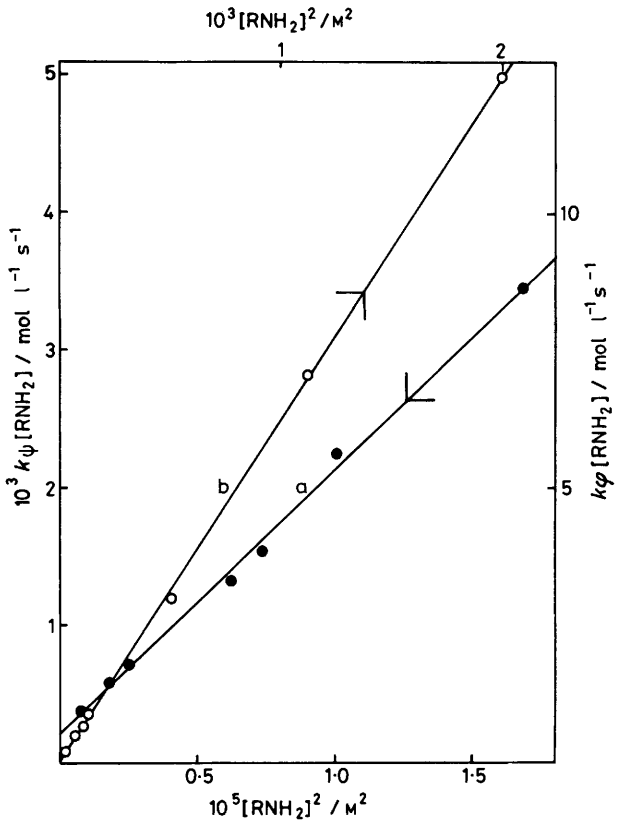

Figure 4. Plot of $k_\varphi[RNH_2]$ against $[RNH_2]^2$ from data of Table 2, part B: a; plot of $k_\psi[RNH_2]$ against $[RNH_2]^2$ from data of Table 3: b

A plot of $[TNA]_0/A_{430}$ against $[RNH_2]^{-2}$ (Figure 3b) is linear. ε_{430} and K_i are 21 000 l mol^{-1} cm^{-1} and 14 400 l mol^{-1}, respectively.

* k_φ and k_ψ symbolize the pseudo-first-order rate constants for stages I and II, respectively, and k_{obs} that for stage III.

Table 3. Reaction of TNA with n-butylamine. Stage II kinetics[a]

$[RNH_2]$/M	k_ψ/s^{-1}
0.000 46[b]	0.147
0.000 76[b]	0.25
0.000 91[b]	0.29
0.001 06[b]	0.34
0.0020[c]	0.60
0.0030[c]	0.94
0.0040[c]	1.25

[a] Temperature: 25 °C; $[RNH_3Cl]$ 0.0050M; measurements were made at 430 nm. [b] $[TNA]_0$ 1.0 × 10^{-5}M. [c] $[TNA]_0$ 3.0 × 10^{-5}M.

Table 4. Reaction of TNA with n-butylamine. Stage III reaction[a]

$[RNH_2]$/M	$[RNH_3Cl]$/M	k_{obs}/s^{-1}	$k_{obs}[RNH_3Cl]^{-1}$/ l mol^{-1} s^{-1}
	Part A		
0.0030	0.0050	0.069	
0.0040	0.0050	0.072	
0.0050	0.0050	0.071	
0.0060	0.0050	0.072	
0.0070	0.0050	0.072	
	Part B[b]		
0.0060	0.0030	0.045	15.0
0.0060	0.0040	0.057	14.3
0.0060	0.0050	0.070	14.0
0.0060	0.0060	0.082	13.7
0.0060	0.0070	0.094	13.4

[a] Temperature: 25 °C; $[TNA]_0$ 3.0 × 10^{-5}M; measurements were made at 430 nm. [b] Data were obtained at constant ionic strength (μ 0.010M) using a compensating electrolyte (tetra-n-propylammonium iodide).

A plot of $k_\psi[RNH_2]$ against $[RNH_2]^2$ (Figure 4b) is also linear.* The slope, k_3, is 310 l mol^{-1} s^{-1}. The straight line passes through the origin, a value of $k_{-3}k_{-4}/k_4$ can not be obtained directly from this plot. The $k_{-3}k_{-4}/k_4$ value of 0.022 s^{-1} is obtained, using $K_i = k_3k_4/k_{-3}k_{-4}$ and the K_i value of 14 400 l mol^{-1}.

Stage III. Kinetics.—The decompostion of the intermediate I^- is much slower than the stage II reaction and its rate can be obtained easily; see trace 1c of Figure 1. This process is rate-limiting in the reaction of TNA and n-butylamine. The pseudo-first-order rate constant, k_{obs}, for the decomposition of the intermediate after the equilibrium between TNA and I^- has been established is given by equation (13). Under the conditions

$$k_{obs} = \frac{k_5K_i[RNH_2]^2[RNH_3^+]}{K_i[RNH_2]^2 + [RNH_3^+]} \quad (13)$$

of $K_i[RNH_2]^2 \gg [RNH_3^+]$ where the equilibrium between TNA and I^- lies almost entirely to the right, this equation reduces to (14).

$$k_{obs} = k_5[RNH_3^+] \quad (14)$$

Kinetic data were obtained by two experiments with the condition $K_i[RNH_2]^2 \gg [RNH_3^+]$ and are given in Table 4. In the first experiment (Part A), the concentration of n-butylamine was varied at a constant concentration of n-butylamine hydrochloride and in the second (Part B), the concentration of n-butylamine hydrochloride was varied at a fixed n-butylamine concentration.

Values of k_{obs} in Part A are almost constant and so the decomposition of I^- is independent of the n-butylamine concentration. On the other hand, values of $k_{obs}/[RNH_3^+]$ in Part B are nearly constant and the decomposition of I^- is first order in n-butylamine hydrochloride.

* In this case, rate equation is given as follows: $k_\psi[RNH_2] = k_3[RNH_2]^2 + k_{-3}k_{-4}[RNH_3^+]/k_4$.

Table 5. Reaction of TNA with n-butylamine. Product equilibrium[a]

$[RNH_2]$/M	A_{500}[b]
0.000 50	0.112
0.000 70	0.134
0.000 90	0.160
0.0070	0.31
0.0101	0.35

[a] Temperature: 25 °C; $[TNA]_0$ 3.0 × 10^{-5}M; $[RNH_3Cl]$ 0.0050M. [b] Equilibrium absorbance at 500 nm; the path length of the cell used is 1 cm.

Table 6. Summary of kinetic and equilibrium results of reaction of TNA with n-butylamine at 25 °C

	Present work	Reaction of methyl 4-methoxy-3,5-dinitrobenzoate with n-butylamine[a]
k_1/l mol^{-1} s^{-1}	3 900 ± 400	
$k_{-1}k_{-2}k_2^{-1}$/s^{-1}	100 ± 10	
K_x/l mol^{-1}	39 ± 7	
k_3/l mol^{-1} s^{-1}	310 ± 20	50
$k_{-3}k_{-4}k_4^{-1}$/s^{-1}	0.022 ± 0.005	38
K_i/l mol^{-1}	14 400 ± 2 000	1.32
k_5/l mol^{-1} s^{-1}	14.1 ± 1.0	470
K_p	4.2 ± 0.7	
K_y/l mol^{-1}	10—21	

[a] From ref. 11.

Product Equilibrium.—In the presence of a low concentration of n-butylamine where the product PH is in equilibrium with only P^-, we tried to obtain a kinetic trace of the formation of P^-. However, we could not obtain any kinetic trace. This indicates that the equilibrium between PH and P^- is attained within the mixing time (1.5 ms) and that, as expected, PH is in rapid equilibrium with P^-.

The equilibrium constants K_p and K_y are defined by equations (15) and (16).

$$K_p = \frac{[P^-][RNH_3^+]}{[PH][RNH_2]} \quad (15)$$

$$K_y = \frac{[Y^-][RNH_3^+]}{[PH][RNH_2]^2} \quad (16)$$

A Benesi–Hildebrand plot[15] (not presented) obtained from the data in Table 5 gives a straight line. ε_{500} and K_p are estimated to be 12 500 l mol^{-1} cm^{-1} and 4.2, respectively.

The K_y value was roughly estimated as follows. The absorption of Y^- can be detected only in the presence of higher concentrations of n-butylamine than 0.020M at 0.0050M-n-butylamine hydrochloride. From equations (15) and (16), (17) is

$$\frac{[Y^-]}{[P^-]} = \frac{K_y[RNH_2]}{K_p} \quad (17)$$

derived. $[Y^-]/[P^-]$ is $0.0048K_y$ at 0.020M-n-butylamine. When $[Y^-]/[P^-]$ is 0.05—0.1, the absorption of Y^- may be detected. Then a K_y value of 10—21 l mol^{-1} is estimated roughly.

The equilibrium and kinetic parameters obtained are summarized in Table 6.

Discussion

Formation of 1,3-*Complex.*—Fyfe *et al.* obtained flow n.m.r. spectra in the reaction of TNA and n-butylamine in methanolic DMSO (50% methanol v/v) and observed that the absorption at δ 8.3 and 5.5 rises to an anomalously high value at the initial stage of the reaction.[5] It was thought that the 1,3-complex X^- was initially produced and that X^-, since it would have a very similar n.m.r. spectrum to that of the 1,3-complex Y^- from amine attack on the product PH, would be indistinguishable from Y^-. Our stopped-flow observations are in accord with those of Fyfe *et al.* The 1,3-complex X^- is produced in the initial stage of the reaction of TNA and n-butylamine.

The rate constant (k_1) for the formation of XH is larger by 12.6-fold than that (k_3) for the formation of IH. The formation of the 1,3-complex is kinetically controlled.

A plot of $[TNA]_0/A_{430}$ against $[RNH_2]^{-2}$ gives a straight line. This indicates that the 1,3-complex exists predominantly as X^- rather than XH.

Proton transfer between XH and X^- is rapid and so the formation of the 1,3-complex is not catalysed by base.

The k_1 value of 4 200 l mol^{-1} s^{-1} obtained from data in Part A of Table 2 agrees well with that of 3 900 l mol^{-1} s^{-1} from Part B. Taking into account the fact that stage I is very fast and so the equilibrium absorbance is an approximation obtained by extrapolating a kinetic trace back to zero time, the K_x value of 27 l mol^{-1} determined from a plot of $[TNA]_0/A_{430}$ against $[RNH_2]^{-2}$ accords with that of 39 l mol^{-1} from a plot of $k_\psi[RNH_2]$ against $[RNH_2]^2$.

Formation and Decomposition of Intermediate.—It has been shown from flow n.m.r. spectroscopy that TNA formed an intermediate complex in the presence of n-butylamine and the kinetic trace due to the intermediate is raised to a maximum between the appearance and disappearance of the product.[5] Our kinetic results also accord with flow n.m.r. spectroscopy.

The equilibrium constant (K_i) for the formation of the intermediate increases by 370-fold, compared with that (K_x) for the formation of the 1,3-complex. The intermediate complex is thermodynamically stable. The increase in equilibrium constant results from the decrease in $k_{-3}k_{-4}/k_4$ [$(k_{-3}k_{-4}/k_4)/(k_{-1}k_{-2}/k_2) = 0.000\,22$].

It is revealed that the intermediate complex is formed *via* the zwitterionic complex IH and proton transfer between IH and I^- is rapid.

The process of the decomposition of the intermediate complex is rate limiting in the overall reaction of TNA with n-butylamine. The decomposition of the intermediate is independent of n-butylamine concentration and first order in n-butylamine hydrochloride. The mechanism of the formation and decomposition of the intermediate is shown to be a rapid equilibrium deprotonation of the zwitterionic complex followed by general acid-catalysed leaving-group expulsion. This is evidence in favour of the SB–GA mechanism of the S_NAr reaction.[8,9,*]

Product Equilibrium.—Fyfe *et al.* have observed that the product is in equilibrium with its 1,3-complex Y^-, formed from amine attack on the product, in the final stage of the reaction.[5] Our observations are different from those of Fyfe *et al.* Our observations are that, in the presence of low concentrations of n-butylamine, P^- is formed from deprotonation of the product PH by n-butylamine and that, in the presence of high concentrations of n-butylamine, the species Y^- is also produced. It is revealed from equation (17) that Y^- is favoured at higher amine concentrations.

Fyfe *et al.* measured in 50% DMSO–50% MeOH and we used DMSO only. It seems that, with increase of DMSO in a solvent mixture, deprotonation of PH becomes more favoured than amine addition.[1b]

Experimental

2,4,6-Trinitroanisole was purified by recrystallization from methanol. *N*-n-Butylpicramide was prepared by reaction of 1-chloro-2,4,6-trinitrobenzene with n-butylamine and recrystallized, m.p. 81 °C (lit.,[17] 82 °C). n-Butylamine, n-butylamine hydrochloride, and tetra-n-propylammonium iodide were prepared as described previously.[10,11] Spectrophotometric grade DMSO and methanol were used as supplied.

Kinetics were carried out at 25 °C using a Union RA 401 stopped-flow spectrophotometer and a Union RA 451 data processor. Rate constants obtained are ordinarily averages of triplicate measurements and are precise to within ±5%. Absorption spectra were recorded on a Hitachi 340 spectrophotometer. Product equilibrium measurements were made by this spectrophotometer.

Acknowledgements

We are grateful to Professor H. Ogino and Dr. Y. Sasaki of Tohoku University for discussions.

References

1 (*a*) M. J. Strauss, *Chem. Rev.*, 1970, **70**, 667; (*b*) F. Terrier, *ibid.*, 1982, **82**, 77.
2 K. L. Servis, *J. Am. Chem. Soc.*, (*a*) 1965, **87**, 5495; (*b*) 1967, **89**, 1508.
3 M. R. Crampton and V. Gold, *J. Chem. Soc. B*, 1966, 893.
4 R. Foster, C. A. Fyfe, P. H. Emslie, and M. I. Foreman, *Tetrahedron*, 1967, **23**, 227.
5 C. A. Fyfe, S. W. H. Damji, and A. Koll, *J. Am. Chem. Soc.*, 1979, **101**, 951.
6 J. A. Orvik and J. F. Bunnett, *J. Am. Chem. Soc.*, 1970, **92**, 2417.
7 J. F. Bunnett, S. Sekiguchi, and L. A. Smith, *J. Am. Chem. Soc.*, 1981, **103**, 4865.
8 (*a*) C. F. Bernasconi, *Acc. Chem. Res.*, 1978, **11**, 147; (*b*) *Chimia*, 1980, **34**, 1.
9 J. F. Bunnett and A. V. Cartaño, *J. Am. Chem. Soc.*, 1981, **103**, 4861.
10 Y. Hasegawa, *Bull. Chem. Soc. Jpn.*, 1983, **56**, 1314.
11 Y. Hasegawa, *J. Chem. Soc., Perkin Trans. 2*, 1984, 547.
12 E. Buncel, M. Hamaguchi, and A. R. Norris, *Can. J. Chem.*, 1980, **58**, 1615.
13 M. R. Crampton and B. Gibson, *J. Chem. Soc., Perkin Trans. 2*, 1981, 533.
14 K. J. Laidler, 'Chemical Kinetics,' McGraw-Hill, New York, 1965, p. 21.
15 H. A. Benesi and J. H. Hildebrand, *J. Am. Chem. Soc.*, 1949, **71**, 2703.
16 M. R. Crampton and P. J. Routledge, *J. Chem. Soc., Perkin Trans. 2*, 1984, 573.
17 M. R. Crampton and B. Gibson, *J. Chem. Soc., Perkin Trans. 2*, 1980, 752.

Received 4th March 1984; *Paper* 4/358

* When our present paper had been submitted, ref. 16 dealing with a similar area was published. A distinct three-stage reaction was also observed in the 2,4,6-trinitrophenetole–n-butylamine system. Our values for kinetic parameters and equilibrium constants for the three-stage reactions are the same order of magnitude as those in ref. 16.